Measure an array of cytokines in COVID-19 samples with our multiplex flow cytometry assays.

Read our app note

BioLegend®

The Journal of Immunology

This information is current as of February 26, 2022.

CD8αα$^+$MHC Class II$^+$ Cell with the Capacity To Terminate Autoimmune Inflammation Is a Novel Antigen-Presenting NK-like Cell in Rats

Jean Wu, Colin Carlock, April Ross, Junbo Shim and Yahuan Lou

J Immunol 2016; 197:4274-4282; Prepublished online 31 October 2016;
doi: 10.4049/jimmunol.1601207
http://www.jimmunol.org/content/197/11/4274

References This article **cites 39 articles**, 13 of which you can access for free at:
http://www.jimmunol.org/content/197/11/4274.full#ref-list-1

Why *The JI*? Submit online.

- **Rapid Reviews! 30 days*** from submission to initial decision
- **No Triage!** Every submission reviewed by practicing scientists
- **Fast Publication!** 4 weeks from acceptance to publication

**average*

Subscription Information about subscribing to *The Journal of Immunology* is online at:
http://jimmunol.org/subscription

Permissions Submit copyright permission requests at:
http://www.aai.org/About/Publications/JI/copyright.html

Email Alerts Receive free email-alerts when new articles cite this article. Sign up at:
http://jimmunol.org/alerts

The Journal of Immunology is published twice each month by
The American Association of Immunologists, Inc.,
1451 Rockville Pike, Suite 650, Rockville, MD 20852
Copyright © 2016 by The American Association of Immunologists, Inc. All rights reserved.
Print ISSN: 0022-1767 Online ISSN: 1550-6606.

Downloaded from http://www.jimmunol.org/ by guest on February 26, 2022

CD8αα$^+$MHC Class II$^+$ Cell with the Capacity To Terminate Autoimmune Inflammation Is a Novel Antigen-Presenting NK-like Cell in Rats

Jean Wu, Colin Carlock,[1] April Ross,[2] Junbo Shim, and Yahuan Lou

Discovery of immune tolerance mechanisms, which inhibit pre-existing autoimmune inflammation, may provide us with new strategies for treating autoimmune diseases. We have identified a CD8αα$^+$MHC class II$^+$ cell with professional APC capacity during our investigation on spontaneous recovery from autoimmune glomerulonephritis in a rat model. This cell actively invades inflamed target tissue and further terminates an ongoing autoimmune inflammation by selective killing of effector autoreactive T cells. In this study, we show that this cell used a cytotoxic machinery of Ly49s$^+$ NK cells in killing of target T cells. Thus, this CD8αα$^+$MHC class II$^+$ cell was a dually functional Ag-presenting NK-like (AP-NK) cell. Following its coupling with target T cells through Ag presentation, killing stimulatory receptor Ly49s6 and coreceptor CD8αα on this cell used rat nonclassic MHC class I C/E16 on the target T cells as a ligand to initiate killing. Thus, activated effector T cells with elevated expression of rat nonclassic MHC class I C/E16 were highly susceptible to the killing by the CD8αα$^+$ AP-NK cell. Granule cytolytic perforin/granzyme C from this cell subsequently mediated cytotoxicity. Thus, inhibition of granzyme C effectively attenuated the killing. As it can recognize and eliminate effector autoreactive T cells in the inflamed target tissue, the CD8αα$^+$ AP-NK cell not only represents a new type of immune cell involved in immune tolerance, but it also is a potential candidate for developing a cell-based therapy for pre-existing autoimmune diseases. ***The Journal of Immunology*, 2016, 197: 4274–4282.**

Most autoimmune diseases are of an inflammatory nature (1, 2). Autoreactive T cells are doubtless the most critical player in these diseases. These T cells function as effectors in both initiation and maintenance of autoimmune inflammation in the target organs (3, 4). Current therapies for those diseases largely rely on nonspecific anti-inflammatory medications, and thus they cannot permanently exterminate the inflammation, and are often accompanied by undesirable serious side effects. Development of immunotherapies that can specifically target autoreactive T cells is a new hope on the horizon for treating inflammatory autoimmune diseases (5). Candidate immune cells for such therapies must be able to specifically silence or terminate a T cell–mediated autoimmune response or inflammation. To discover and elucidate novel immune tolerance mechanisms are prerequisites for identifying such candidate immune cells.

Many types of immune cells (e.g., regulatory T cells, immature or tolerogenic dendritic cells [DCs], and a subset of NK cells) have been candidates for immunotherapies (6–9). These cells reside in lymphoid organs or normal tissues and eliminate naive autoreactive T cells or deviate them to a nonpathogenic phenotype. Thus, generation of effector autoreactive T cells and subsequent autoimmune inflammation are prevented de novo. However, pathogenic autoreactive T cells can evade these tolerance mechanisms through molecular mimicry or bystander activation during infections (10, 11). Are there any last-ditch tolerance mechanisms that suppress autoimmunity after pathogenic autoreactive T cells have caused or are causing tissue damage? To address this fundamental question is critical for both our full understanding of immune tolerance and development of immunotherapies. Clinically, it is difficult to detect autoimmune diseases before their onset. A practical therapy is to suppress a pre-existing disease rather than to prevent them. Therapeutic strategies based on many tolerance mechanisms may successfully prevent the diseases, but they are less effective for treating a pre-existing disease.

During our investigation on spontaneous recovery from autoimmune glomerulonephritis in Lewis (LEW) rats, a population with a CD8αα$^+$MHC class II (MHC-II) B and D loci (RT1B/D)$^+$ phenotype and professional APC capacity has been identified (12–14). This population expands upon autoimmunization and migrates into inflamed target tissue (13). Their Ag presentation induces apoptosis in effector autoreactive T cells in the target tissue, leading to a spontaneous recovery (14). We have linked migration deficiency to disease susceptibility in the disease-prone Wista Kyoto (WKY) rats. Significantly, transfer of this cell population of LEW rats attenuates pre-existing disease in WKY rats (15). This suggests that the CD8αα$^+$RT1B/D$^+$ cell is a potential candidate for immunotherapy for a pre-existing autoimmune disease. The present study sought to investigate cytotoxic mechanisms in the CD8αα$^+$RT1B/D$^+$ cell. Our results showed that the CD8αα$^+$ RT1B/D$^+$ cell was an unusual Ag-presenting NK-like cell: it engages

Department of Diagnostic Sciences, University of Texas Health Science Center at Houston, Houston, TX 77054

[1]Current address: Department of Biochemistry, Purdue University, West Lafayette, IN.

[2]Current address: Department of Immunology, University of Texas M.D. Anderson Cancer Center, Houston, TX.

ORCID: 0000-0002-4219-5526 (J.S.).

Received for publication July 12, 2016. Accepted for publication October 4, 2016.

This work was supported by National Institutes of Health Grants R01 DK60029 and R01 DK077857 (to Y.L.), as well as by a National Institutes of Health supplemental grant (to A.R.).

Address correspondence and reprint requests to Dr. Yahuan Lou, Department of Diagnostic and Biomedical Sciences, School of Dentistry, University of Texas Health Science Center at Houston, 5326 Behavioral and Biomedical Science Building, 1941 East Road, Houston, TX 77054. E-mail address: Yahuan.lou@uth.tmc.edu

Abbreviations used in this article: AP-NK, Ag-presenting NK-like; DC, dendritic cell; Gzm, granzyme; ISH, in situ hybridization; LEW, Lewis; MHC-I, MHC class I; MHC-II, MHC class II; qPCR, quantitative PCR; RT, reverse transcription; RT1B/D, rat MHC class II B and D loci; RT1CE, rat nonclassic MHC class I C/E16; WKY, Wista Kyoto.

Copyright © 2016 by The American Association of Immunologists, Inc. 0022-1767/16/$30.00

www.jimmunol.org/cgi/doi/10.4049/jimmunol.1601207

Downloaded from http://www.jimmunol.org/ by guest on February 26, 2022

with and recognizes autoreactive effector T cells as an APC, and further kills them as an NK cell.

Materials and Methods

Rats and induction of glomerulonephritis

All procedures involving animals in this study were approved by the Institutional Animal Welfare Committee. Female WKY or LEW rats (4–6 wk of age) were purchased from Harlan Laboratories (Indianapolis, IN). Rats were immunized with peptide pCol(28–40) (0.15 μmol) emulsified in CFA in one hind footpad and at the base of the tail (10). Development of proteinuria in these rats was closely monitored daily. Immunized rats were then used for the isolation of various leukocyte populations at days 30–35 depending on their status of proteinuria. Peripheral blood and kidneys were removed under sterile conditions for cell isolation. A portion of renal tissues was either snap frozen or fixed for evaluation of renal pathology. In some cases, immunized rats were perfused with 2% paraformaldehyde for in situ hybridization.

Antibodies

Biotin-labeled anti-rat CD3 (G.4.18), PE-labeled anti-rat CD4 (OX35), CD8α (OX8), CD11c, RT1B (OX6), FITC-labeled anti-rat CD8α, RT1B (OX6), RT-1D (OX17), and allophycocyanin-labeled CD8α were from BD Biosciences (San Diego, CA). Goat anti-CD34, CD94, rat NK marker (ANK61), and anti-rat granzyme (Gzm) C were from Santa Cruz Biotechnology (Sana Cruz, CA). Anti-rat CD32 (D34-485) was used for Fc block. PE, FITC, anti-rat IgG, and purified rat IgG were from SouthernBiotech (Birmingham, AL). Various mouse Ig isotypes (BD Biosciences) and normal rat/mouse IgG (SouthernBiotech) were used as controls in both flow cytometry and immunofluorescence. Anti-Ly49s antiserum was generated through immunization of mice with a synthetic 16-mer peptide of a conserved region of Ly49s receptors (DCGKRYLCICEKGMDK). Sera from mice immunized with adjuvant alone or an irrelevant peptide were used as negative controls.

Isolation and characterization of CD8αα$^+$RT1B/D$^+$ cells

PBMC fractions were first isolated from immunized rats by Ficoll gradient centrifugation. Glomeruli were purified from immunized rats and digested to release glomeruli-infiltrating leukocytes following a previously established method (14, 15). The cells were subjected to isolation of various cell populations on a magnetic beads–based automatic cell sorter (Miltenyi Biotec, Bergisch Gladbach,Germany). Pan T cells were first removed by a pan T cell isolation kit from Miltenyi Biotec. CD8α$^+$ cells were then positively selected and further fractionated into RT1B/D^{high} and RT1B/D^{low} populations using a combination of removable antifluorescence Ab and FITC–anti-RT1B/D Ab (Miltenyi Biotec). All populations were then analyzed for their purities by three-color flow cytometry (CD8α versus RT1B/D versus CD3). CD8α$^+$ RT1B/D^{low} cells were further analyzed with two Abs to rat NK cells. A total of 11 isolations were performed. Only those with purities >93% were used for DNA microarray studies. Cells were either immediately used for isolation of total RNA or fixed for immunofluorescence and in situ hybridization. Glomeruli-infiltrating CD8α$^-$RT1B/D$^+$ cells were considered as infiltrating macrophages. Thus, in addition to CD8αα$^+$RT1B/D$^+$ cells, the following populations were also obtained as controls: PBMC pan T cells, glomeruli-infiltrating macrophages, and pan T cells.

Rat DNA microarray assay

Total RNA from various cell populations was isolated with a kit (Ambion, Austin, TX) and checked for its quality. Three hundred nanograms of total RNA was amplified and purified using an Illumina TotalPrep RNA amplification kit (Illumina, San Diego, CA) following the manufacturer's instructions. RNase H and DNA polymerase master mix were immediately added into the reaction mix following reverse transcription (RT) and were incubated for 2 h at 16°C to synthesize second-strand cDNA. In vitro transcription was performed, and biotinylated cRNA was synthesized by 14 h of amplification with 2′-deoxynucleoside 5′-triphosphate mix containing biotin–deoxyuridine triphosphate and T7 RNA polymerase. Amplified cRNA was subsequently purified and the concentration was measured by a NanoDrop ND-1000 spectrophotometer (NanoDrop Technologies, Wilmington, DE). An aliquot of 750 ng of amplified products was loaded onto Illumina Sentrix BeadChip array rat arrays, hybridized at 58°C in an Illumina hybridization oven for 17 h, washed, and incubated with streptavidin-Cy3 to detect biotin-labeled cRNA on the arrays. Arrays were dried and scanned with a BeadArray Reader (Illumina). Data were analyzed using GenomeStudio software (Illumina). Clustering and pathway analyses were performed with GenomeStudio and Ingenuity Pathway Analysis (Ingenuity Systems, Redwood City, CA) softwares, respectively. DNA microarray megadata have been published (access no. GSE87099; http://www.ncbi.nlm.nih.gov_geo).

RT-PCR, molecular cloning, and in situ hybridization

Total RNAs from various cell populations were used for RT-PCR. cDNA was synthesized using 1 μg of total RNA through an RT kit (RNA PCR core kit; Applied Biosystems, Foster City, CA). Primers for various PCRs are listed in Table I. Quantitative PCR (qPCR) for rat nonclassic MHC class I C/E16 (RT1CE) on various T cells was performed under a similar condition as for conventional PCR using a SYBR Green system (SuperArray Bioscience, Frederick, MD) on an iCycler iQ thermocycler (Bio-Rad Laboratories, Hercules, CA). Relative abundance was calculated as $2^{\Delta(t\ -\ t_0)} \times 100$ (%) with activated T cells or *Gapdh* as t_0. RNAs from isolated glomeruli of WKY rats at days 20 and 30 postimmunization were used for RT^2 Profiler PCR array rat apoptosis (Qiagen, Hilden, Germany) following the manufacturer's instructions. For cloning of full-length rat *gzm c*, full-length *ly49s6*, and degenerative cloning of intracellular/transmembrane domain of Ly49 receptors, RNA from glomeruli-infiltrating CD8αα$^+$RT1B/D$^+$ cells was used. RT-PCR products were cloned into pCR-Blunt II-TOPO vector (Invitrogen, Carlsbad, CA). Insert DNA from each clone was sequenced with either forward or reverse M13 promotor (Integrated DNA Technologies, Coralville, IA). For in situ hybridization (ISH), paraformaldehyde-fixed cells or perfused renal tissues were used. Sense and antisense RNA for rat *gzm c* were transcribed from linearized plasmid containing full-length rat *gzm c* with a transcription kit (MEGAscript T7; Ambion), using T7 or SP6 RNA polymerase, respectively; biotin-UTP was added at 25% of total UTP for labeling of RNA probes. Biotin-labeled RNA probes were then used for SSC/Denhardts-based hybridization at 37°C with an RNA probe (400 ng/ml) in an ISH moisture chamber. After hybridization, cells or tissues were incubated with streptavidin–Texas Red, followed by immunofluorescence for RT1B/C or CD8α.

Immunofluorescence and flow cytometry

Fixed or live cells were used for immunofluorescence or flow cytometry following our previously published methods (12). For flow cytometry, standard controls included Ig isotypes and fluorescence minus one. For detection of intracellular Fas-L or Gzm C, cells were permeablized with a regent (intracellular cytokine detection kit; BD Biosciences) before staining. All sections or cells were counterstained by DAPI and observed with a digital fluorescent confocal microscope (Eclipse 80i; Nikon, Tokyo, Japan). Digital images were recorded for evaluation. Stained cells were also analyzed by flow cytometry following our established method (14).

In vitro killing assays

T cell lines specific to pCol(28–40) were generated following our established method (14). Resting or activated T cells were used as target cells. For activation, T cells were incubated with irradiated thymic APC and pCol(28–40) at a suboptimal concentration (3 μM) for 48 h (14). In either case, T cells were then labeled by CFSE (15). Glomeruli-infiltrating CD8αα$^+$RT1B/D$^+$ were isolated as described above and used as killing effectors. To each round-bottom well of a 96-well plate, 10^5 labeled T cells and 10^5 CD8αα$^+$RT1B/D$^+$ cells were added in the presence of 10 μM pCol (28–40). In some cases, an Ab (2 μg/ml) or normal IgG was added as indicated. Wells with T cells alone were used as a baseline for T cell numbers. Each set of incubation was duplicated. The remaining T cells were counted under a fluorescence microscope at 72 h, and killing efficacy for each well was calculated as ratio (percentage) between T cell numbers of a testing well versus a T cells alone well.

Statistical analysis

Linear progression or nonpaired *t* tests were performed for comparison between various experimental results. One-way ANOVA with a Tukey posttest was used for comparison among more than two groups. Linear regression was used to analyze RT1CE16 expression and killing efficacy. A p value <0.05 was considered significant.

Results

A distinct global gene expression pattern of CD8αα$^+$RT1B/D$^+$ cells

We have shown a small size of the CD8αα$^+$MHC-II(RT1B/D)$^+$ population in both PBMCs and glomeruli-infiltrating leukocytes. A special magnetic beads–based cell sorting was first developed to maximize the purity and to minimize the damage to the cells (Fig. 1A, 1B). Two subpopulations, CD8αα$^+$RT1B/D^{high} and CD8αα$^+$RT1B/D^{low}, were obtained from each source (Fig. 1B). The separation into two subpopulations ensured freedom from

Downloaded from http://www.jimmunol.org/ by guest on February 26, 2022

potential contamination of CD8$^+$ MHC-II$^-$ cells such as cytotoxic T, NK, or γδT cells in the CD8αα$^+$RT1B/D^{high} subset. Glomeruli-infiltrating macrophages and T cells and PBMC T cells from the same individual were used as controls for comparisons (Fig. 1B). Global gene expression patterns of various CD8αα$^+$RT1B/D$^+$ subpopulations were analyzed by two independent DNA microarrays, with each containing two independent samples (total of four) for each subpopulation. Both microarrays showed that all CD8αα$^+$RT1B/D$^+$ subpopulations clustered together tightly (Fig. 1C), suggesting a similarity in their gene expression pattern. In contrast, glomeruli-infiltrating macrophages and pan T cells showed very distinct expression patterns (Fig. 1C). Thus, all CD8αα$^+$ RT1B/D$^+$ subpopulations likely belonged to a single population, probably at different activation status. We used the CD8αα$^+$ RT1B/D^{high} subpopulation for most experiments in this study unless indicated otherwise. These cells are referred to as CD8αα$^+$ RT1B/D$^+$ cells.

CD8αα$^+$RT1B/D$^+$ cells express genes associated with professional APCs and NK cells

We have previously reported that APC function of the CD8αα$^+$RT1B/D$^+$ cell is a prerequisite for induction of apoptosis in effector T cells (14). We analyzed the DNA microarray data for the expression of gene clusters, which are associated with professional APC- and apoptosis-related cytotoxicity. The CD8αα$^+$RT1B/D$^+$ cells expressed both professional APC- and NK cell–specific genes (Fig. 1D). These APC-related genes included MHC-II *rt1b/d/m*, invariant chain *li/clip*, and protease cathepsins, which are specific for Ag processing/presentation in professional APCs (Fig. 1E). The expression pattern of these genes in the CD8αα$^+$RT1B/D$^+$ cells was very similar to that of glomeruli-infiltrating macrophages, although the expression levels were lower (Fig. 1E). RT-PCR on selected genes demonstrated that both CD8αα$^+$RT1B/D^{high} and CD8αα$^+$RT1B^{low} subsets expressed *rt1bα* and *Clip/li* (Fig. 1F) (Table I). Thus, the CD8αα$^+$RT1B/D$^+$ cells possessed Ag processing/presentation apparatus for a professional APC, as we have previously reported (14, 15). In fact, both α- and β-chains of *rt1b* and *rt1d* have been cloned from the CD8αα$^+$ RT1B/D$^+$ cells (GenBank AY701537–AY701540). We next analyzed the expression of NK-associated genes, that is, various NK killing stimulatory/inhibitory receptors, associated signaling proteins such as DAP12, and granule cytolytic proteins in the CD8αα$^+$RT1B/D$^+$ cells. The CD8αα$^+$RT1B$^+$ cells expressed nearly half of these genes at a significant level (Fig. 1D). Also, note that the cells expressed an extremely high level of *Tyrobp* (Fig. 1D), which encodes DAP12, a known critical signaling molecule for killing receptor-mediated cytotoxicity in NK cells (16). The expression of DAP12 was further verified by RT-PCR (Fig. 1D, inset). Thus, the CD8αα$^+$RT1B/D$^+$ cells also expressed genes associated with NK cytotoxicity.

CD8αα$^+$RT1B/D$^+$ cells express NK killing stimulatory receptor Ly49s6 and cytolytic proteins

Three groups of molecules, that is, killing activating/inhibitory receptors, granule cytolytic proteins, and Fas-L, are associated with NK cytotoxicity (17). First, we focused on the NK receptors.

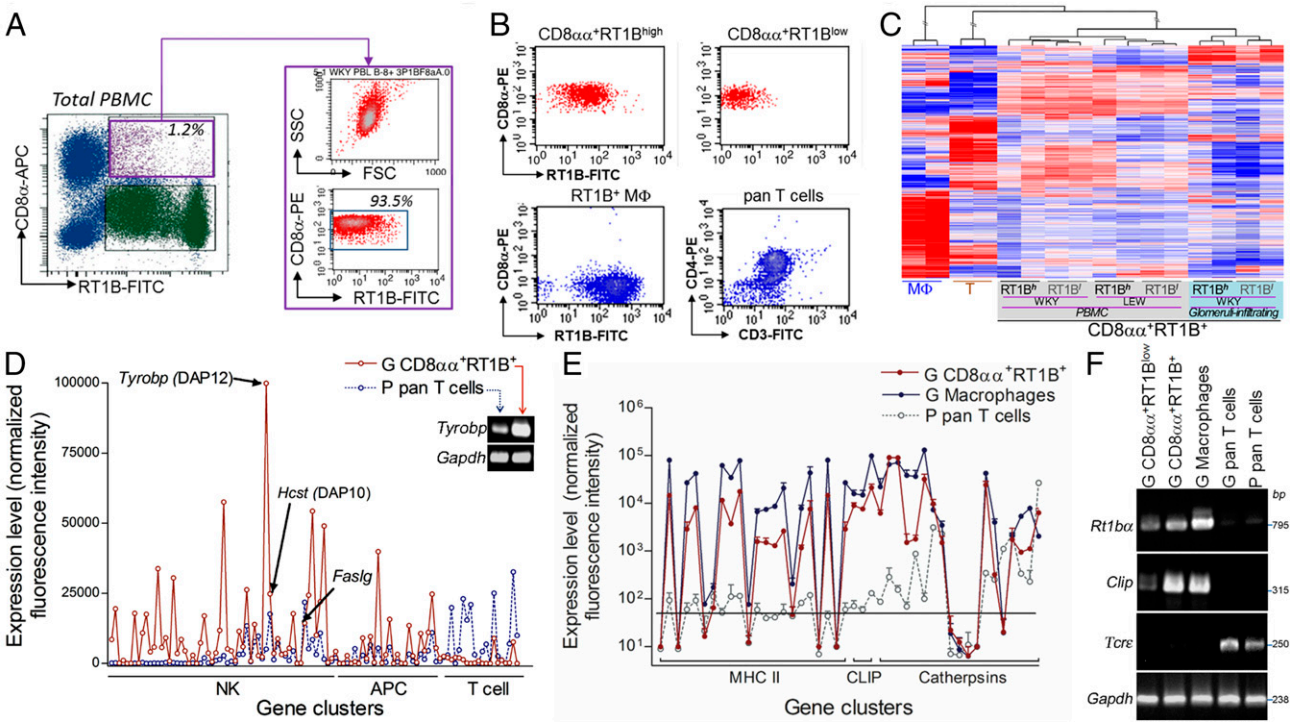

FIGURE 1. CD8αα$^+$RT1B/D$^+$ cells express both genes associated with professional Ag processing/presenting and NK cytotoxicity. (**A**) Multicolor flow cytometry analyses show a CD8αα$^+$RT1B/D$^+$ population (purple gate on RT1B-FITC versus CD8α-APC plot, left panel) in rat PBMCs; the right panel shows the purified CD8αα$^+$RT1B/D$^+$ population as shown by both side light scatter (SSC) versus forward light scatter (FSC) and CD8α versus the RT1B/D plot. (**B**) Representative flow cytometric plots show each isolated population from glomeruli-infiltrating leukocytes as indicated on the top of each plot. MΦ, macrophage. (**C**) A representative clustering analysis based on DNA microarray shows similar global gene expression patterns among all CD8αα$^+$RT1B/D$^+$ subpopulations from different sources in both LEW and WKY rats; glomeruli-infiltrating macrophages (MΦ) and pan T cells are shown as controls. (**D**) Summary of expressions of gene clusters associated with NK cells, APCs, and T cells (n = 4). Inset, RT-PCR detection of *Tyrobp* and the control housekeeper gene *Gapdh*. (**E**) Summary of expressions of genes associated with Ag processing/presentation for professional APCs; expression levels in (D) and (E) are mean normalized intensities for each gene in the DNA microarray (n = 4). (**F**) A representative RT-PCR shows expression of an Ag presenting–related α-chain of rat MHC-II RT1B (*Rt1bα*) and invariant chain (*Clip*) in various cell populations as indicated; the TcR ε-chain (*Tcrε*) and *Gapdh* were used as controls.

Downloaded from http://www.jimmunol.org/ by guest on February 26, 2022

Table I. PCR primers used for detection of expression of various genes or cloning of cDNAs

Rat Gene	Primers	Product Size (bp)
Rt1bα	F, 5′-AGAACAGAGATGCCGCTCAGCAGAGC-3′ R, 5′-TTCCCAGGATGGTACTCAAAGGGGCC-3′	795
Clip (Il)	F, 5′-TGTTCTTGTGAAGACAGAAGCCAGC-3′ R, 5′-GTATCCAGCCTAGATTAAGGGTAGG-3′	315
Tcrε	F, 5′-GGTACTGGTGGCAGGCCCAGAGG-3′ R, 5′-GTTCTAGGATGCGTGTTCACCAGG-3′	250
Gapdh	F, 5′-CTTCACCACCATGGAGAAGGC-3′ R, 5′-GGCATGGACTGTGGTCATGAG-3′	238
Tyrobp	F, 5′-GCTTCAGGGTCAGAGGCCAGAA-3′ R, 5′-TGGGGACAGAAACGGTACAAGG-3′	218
Ly49s3	F, 5′-GTCTGTATTTCAGTATGTCAGG-3′ R, 5′-ATTCTCCACATGCAAGCTCCTC-3′	236
Ly49s4	F, 5′-GTATGTATTTCAGTATGTCAGG-3′ R, 5′-TCACACAGCAGAATGTGACC-3′	135
$Ly49s5_{ORF}$	F, 5′-TCCCAAAATGAGTAAGCAGGATG-3′ R, 5′-ATCATCTCTCTATTCACACAGCAG-3′	854/741
Ly49s6	F, 5′-CTCCCAAAATGAGTAAGCAGG-3′ R, 5′-CATCTCTTTATTCACAGAGCAG-3′	614
$Ly49_{TM/IC}$	F, 5′-ACAGACTTCATACATCATTCCC-3′ R, 5′-AACAGCAACCAGCCGAAG-3′	199/208
Gzma	F, 5′-CTGGGTGTCCTCTCTTACTACTGTC-3′ R, 5′-TTAAACAGCGCCCTTCGCAGTCTTC-3′	766
Gzmb	F, 5′-TTTCCTAGAGGTGAAGAGAGCAAGG-3′ R, 5′-AGGGCAGATGGTTAGTCAGGAAATG-3′	860
$Gzmc_{ORF}$	F, 5′-GAGGATGCCACCAGTCCTGATACTC-3′ R, 5′-GCTATAGGGAAGATGGTTAGTCAGG-3′	800
Pfr	F, 5′-CTCAAGCGAATACAAAGCTTGCGAGG-3′ R, 5′-TTGTTTTTACCACACAGCCCCACTGC-3′	859
Rt1ce5	F, 5′-CCTTCCACATTCAACCTTGCTG-3′ R, 5′-TGTAGAAGTGAGGAGTTGCAG-3′	103
Rt1ce14	F, 5′-CCTTCCAGAAGTGGGCATCTGT-3′ R, 5′-ATGGCCACAGCTCCAATGATGG-3′	211
Rt1ce16	F, 5′-GCAGTTGAATGGGGAGGACC-3′ R, 5′-ATCACAACAGCCACCACAGC-3′	286
Faslg	F, 5′-AAAGACCACAAGGTCCAACA-3′ R, 5′-AGTCTCTAGCTTATCCCATGA-3′	341
Lat	F, 5′-CCCACACAGACGGCATCTCC-3′ R, 5′-CTGAGCATCTGGAGTGGCCC-3′	210

F, forward; R, reverse.

Two NK cell subsets, that is, Ly49$^+$ and NKR-P1B$^+$, have been identified in rats (18). The microarray revealed a predominant expression of the NK receptor *Ly49* family, but not the *Klrb1* family, in CD8αα$^+$RT1B$^+$ cells (Fig. 2A). The cells especially lacked the expression of *Klrb1b*, which encodes hallmark NKR-P1B for the NKR-P1B$^+$ subset. Thus, the NK receptor expression pattern of CD8αα$^+$RT1B/D$^+$ cells resembled that of the Ly49s$^+$ subset. The rat Ly49 family has at least 35 members, and their complicated expression pattern is associated with the host's MHC haplotypes (19). Furthermore, most of them have not been studied or cloned in rats. RT-PCR indeed revealed a complicated expression pattern in CD8αα$^+$RT1B/D$^+$ cells, including splice variants (Fig. 2B). However, PCR results did not match those from the microarray, because the microarray covered only a few known Ly49 receptors from the PVG strain. Additionally, similarity among Ly49 members may have led to cross-reactivity. Thus, both PCR and the microarray data may not accurately reflect real expression of Ly49 NK receptors. We decided to analyze the intracellular/transmembrane domain of Ly49s, which determines whether engagement of a receptor leads to killing activation or inhibition. Degenerative cloning of the transmembrane/intracellular domain of Ly49 was performed with mRNA from the CD8αα$^+$ RT1B/D$^+$ cells (Fig. 2B, lower panel). Amino acid sequences from 33 clones were then compared with known stimulatory or inhibitory Ly49 receptors (19, 20). All of these sequences belonged to stimulatory receptors, with 18 being Ly49s6. No T-TYT-H motif for inhibitory receptors was observed in these clones (20). Cloning of full-length cDNA from the CD8αα$^+$RT1B/D$^+$ cell showed that it was a novel splice variant of killing stimulatory Ly49s6 with the addition of nine nucleotides (cDNA sequence in GeneBank: KX501213.1) (Fig. 2C). With an Ab against the C-terminal region of Ly49s6, coexpression of surface Ly49s6 and RT1B/D was demonstrated on the CD8αα$^+$RT1B/D$^+$ cells by both immunofluorescence and flow cytometry (Fig. 2D, 2E). These results provided direct evidence for the coexpression of NK- and professional APC–specific molecules in the CD8αα$^+$RT1B/D$^+$ cells. Thus, the phenotype of this cell is CD8αα$^+$RT1B/D$^+$Ly49s6$^+$.

Second, we investigated the expression of cytolytic granule proteins. RT-PCR detected abundant mRNAs for perforin and *gzm* in the CD8αα$^+$RT1B/D$^+$Ly49s6$^+$ cells (Fig. 3A). Unlike NK and CD8$^+$ T cells, the CD8αα$^+$RT1B$^+$Ly49s6$^+$ cells preferentially expressed *gzm c* (Fig. 3A). cDNA encoding the full length of *gzm c* (248 aa with a molecular mass of 28 kDa) was cloned from CD8αα$^+$RT1B$^+$Ly49s6$^+$ cells (GenBank: KT878764.1). Sequencing of independent clones confirmed it to be rat *gzm c*. ISH combined with immunofluorescence revealed *gzm c* mRNA in PBMCs and glomeruli-infiltrating CD8αα$^+$RT1B$^+$Ly49s6$^+$ cells (Fig. 3B–D). Three-color immunofluorescence (RT1B, CD8α, and Gzm C) demonstrated cytoplasmic Gzm C protein in these cells (Fig. 3E). Western blot detected Gzm C as a 56-kDa protein instead of the predicted 28 kDa (Fig. 3F). Gzm C is much less studied, and its native tertiary structure remains unclear. Our result agreed with a previous x-ray study that native Gzm C is a homodimer (21). Glomeruli-infiltrating CD8αα$^+$RT1B$^+$Ly49s6$^+$ cells, which were

Downloaded from http://www.jimmunol.org/ by guest on February 26, 2022

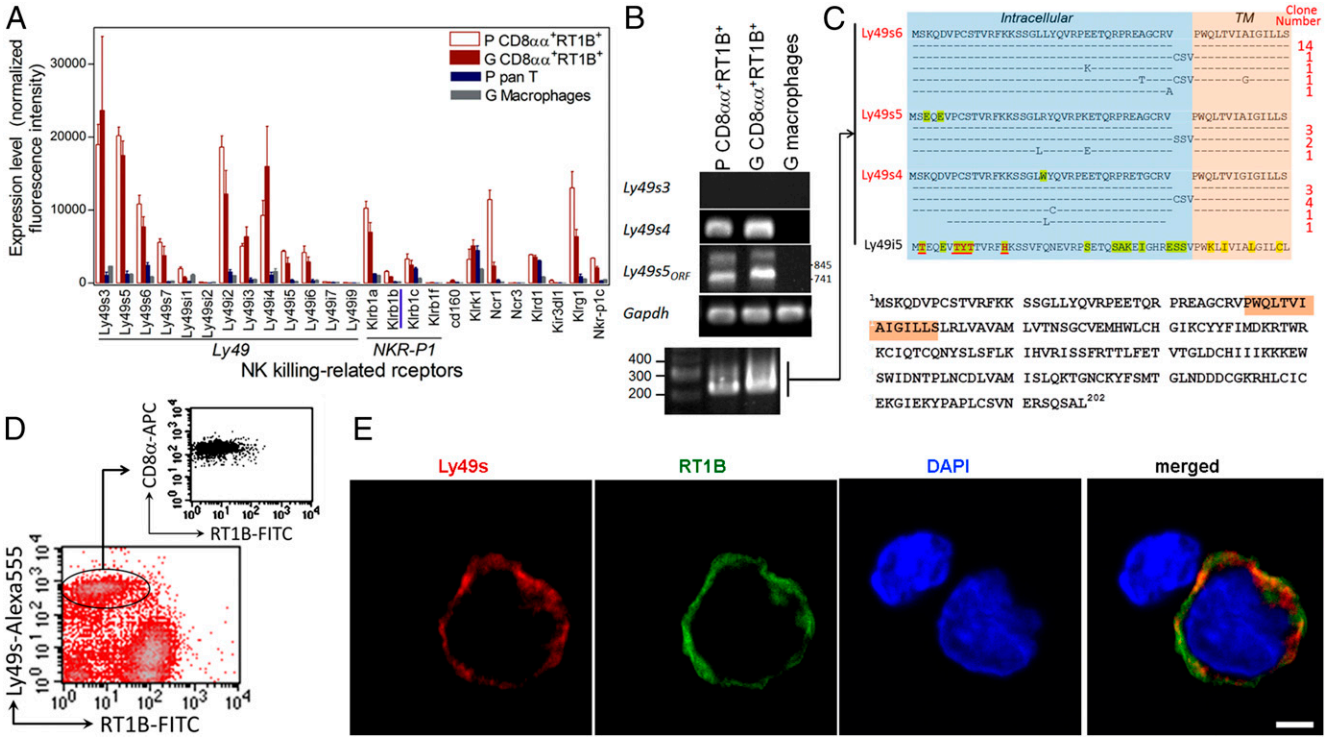

FIGURE 2. CD8αα$^+$RT1B/D$^+$ cells express the NK killing stimulatory receptor Ly49s6. (**A**) DNA microarray shows expression of various NK receptors in PBMC (P) and glomeruli-infiltrating (G) CD8αα$^+$RT1B/D$^+$ cells, but not in control PBMC T cells and glomeruli-infiltrating macrophages; NK receptor genes are grouped; the gene *Klrb1a*, which encodes a hallmark of an NK subset NKR-P1B, is underlined; note that many Ly49 members were not covered by the DNA microarray. (**B**) RT-PCR detection of mRNAs for representative Ly49 receptors in the indicated cell populations; the lower panel shows degenerative PCR products for transmembrane (TM) and intracellular fragments of Ly49 in glomeruli-infiltrating CD8αα$^+$RT1B/D$^+$ cells. (**C**) Alignment of amino acid sequences of cloned cDNA from degenerative PCR [see lower panel in (B) as connected by lines] demonstrates expression of mainly killing stimulatory receptors in CD8αα$^+$RT1B/D$^+$ cells; the numbers of clones for each sequence are indicated at the right, with most of them being Ly49s6; the inhibitory motif in the intracellular fragment of Ly49 is underlined in red at the bottom. *TM*, transmembrane. The lower panel shows the amino acid sequence of cloned Ly49s6 with the transmembrane domain shadowed. (**D**) Three-color flow cytometry on glomeruli-infiltrating leukocytes after removal of pan T cells shows an RT1B/D$^+$ Ly49s6$^+$ population (lower panel) that is also CD8α$^+$ (upper panel for the gated population in lower panel). (**E**) Immunofluorescence shows expression of both Ly49s6 (red) and RT1B (green) on a CD8αα$^+$RT1B/D$^+$ cell; a nearby T cell is shown as an internal control for staining. Scale bar, 3 μm.

T cell killers, showed a much higher level of Gzm C protein than found in other subpopulations (Fig. 3F).

Third, simultaneous expression of Fas-L with other cytotoxicity-related genes in NK or cytotoxic T cells is well known. We next asked whether Fas-L was also expressed in the CD8αα$^+$RT1B$^+$Ly49s6$^+$ cells. With purified glomeruli from immunized rats, a qPCR array for the apoptotic pathway revealed a 15-fold increase in glomerular *Faslg* expression at day 35 (the peak time for T cell apoptosis in glomeruli) as compared with day 20 (early inflammation) (13) (Fig. 4A). RT-PCR using fractionated cell populations demonstrated that the glomeruli-infiltrating CD8αα$^+$RT1B$^+$Ly49s6$^+$ cells were the source of glomerular *fasgl* but not *LTα* (Fig. 4B). Flow cytometry on freshly purified glomeruli-infiltrating CD8αα$^+$RT1B$^+$ Ly49s6$^+$ cells failed to detect Fas-L. However, permeabilization of the cells led to detection of Fas-L in 68% of these cells (Fig. 4C), suggesting the presence of intracellular Fas-L. Similarly, immunofluorescence detected Fas-L only in permeabilized CD8αα$^+$RT1B$^+$ Ly49s6$^+$ cells (Fig. 4D). Intracellular Fas-L has been described as a "safe storage" through posttranslational modification, which is ready for mobilization upon stimulation (22).

Cytolytic Gzm C in CD8αα$^+$RT1B$^+$Ly49s6$^+$ cells mediates killing of autoreactive T cells

The above results demonstrated that the CD8αα$^+$RT1B$^+$Ly49s6$^+$ cell possessed both NK killing receptors/cytolytic granules and intracellular Fas-L. We next determined which pathway played a major role in killing autoreactive T cells. Three autoreactive T cell lines specific to autoantigen pCol(28–40) were activated with irradiated thymic APCs and pCol(28–40) for 48 h; the T cells were harvested and labeled with CFSE as target cells. The target T cells were incubated with freshly isolated glomeruli-infiltrating CD8αα$^+$RT1B$^+$ Ly49s6$^+$ cells as killing effectors in the presence of pCol(28–40). Anti–Fas-L Ab or normal IgG was added to the killing test. Interestingly, the Ab slightly, but not significantly, enhanced T cell apoptosis instead of inhibition (Fig. 4E). With a similar killing assay, addition of anti–Gzm C Ab led to a significant reduction in T cell death from 81 to 29% (Fig. 3G). In both cases, IgG controls did not affect the killing. Thus, NK granular cytolytic pathway, but not Fas-L, was the major player in mediating apoptosis in T cells.

Elevated expression of nonclassic MHC class I RT1CE16 on activated autoreactive T cells coincides with their higher susceptibility to CD8αα$^+$RT1B$^+$Ly49s6$^+$ cell–mediated apoptosis

Because degranulation is triggered by killing stimulatory receptors, we asked whether killing stimulatory Ly49s6 on the CD8αα$^+$RT1B$^+$Ly49s6$^+$ cells initiated the killing. It is known that the ligands for Ly49 are nonclassic MHC class I (MHC-I) molecules including RT1CE on the target cells (20, 23). The CD8αα homodimer preferentially binds to nonclassic MHC-I molecules and may serve as a coreceptor (24). Expression of the nonclassic MHC-I gene cluster (25) on glomeruli-infiltrating pan T cells and PBL pan T cells was compared (Fig. 5A). Glomeruli-infiltrating pan T cells were largely CD4$^+$ effector autoreactive T cells. Alternatively, PBL pan T cells were a mixture with most being nonactivated T cells

Downloaded from http://www.jimmunol.org/ by guest on February 26, 2022

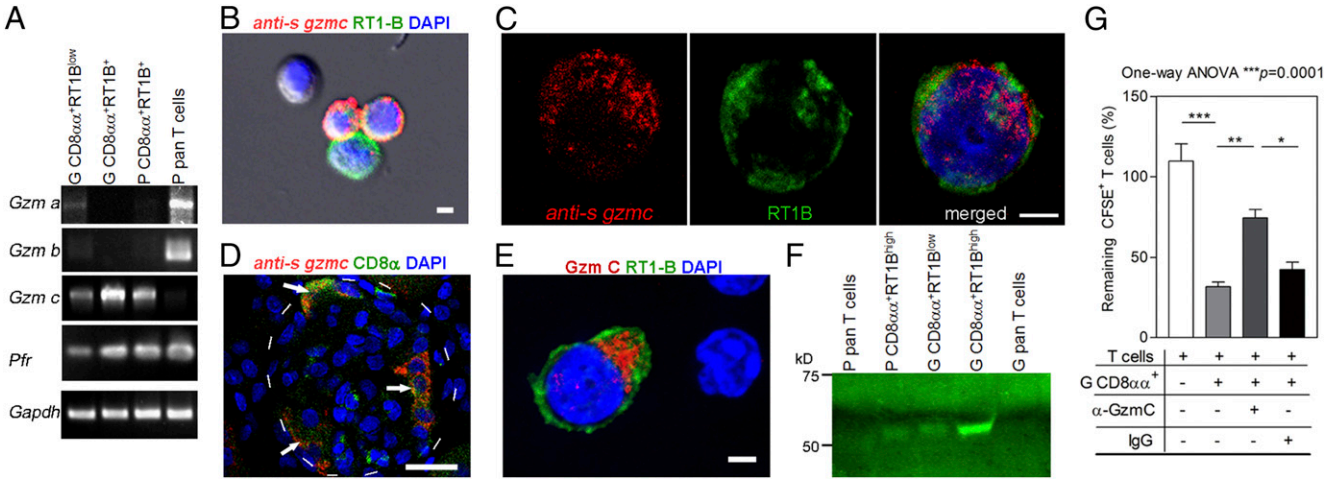

FIGURE 3. Granule cytolytic Gzm C in CD8αα$^+$RT1B/D$^+$Ly49s$^+$ cells mediates killing of autoreactive effector T cells. (**A**) RT-PCR detection of granule cytolytic proteins in various cell populations. (**B** and **C**) Combination of immunofluorescence on RT1B (green) and ISH with full-length *gzm c* antisense RNA (anti-s) as a probe (red) demonstrate *gzm c* mRNA in CD8αα$^+$RT1B/D$^+$Ly49s6$^+$ PBMCs; cells probed with sense RNA were negative. In (B), one double-negative and one single RT1B/D$^+$ cell (green) are shown as internal controls. Scale bars, 3 μm. (**D**) Immunofluorescence/ISH show *gzm c* mRNA in CD8αα$^+$ RT1B/D$^+$Ly49$^+$ cells (arrows) in glomeruli (outlined by dashed line) of an immunized rat. Scale bar, 30 μm. (**E**) Immunofluorescence shows cytoplasmic Gzm C (red) in a glomeruli-infiltrating CD8αα$^+$RT1B/D$^+$Ly49s$^+$ cell (green); two nearby double-negative T cells are shown as internal controls. Scale bar, 3 μm. (**F**) Western blot on the proteins from various cells shows Gzm C of 56 kDa in CD8αα$^+$RT1B/D$^+$Ly49s$^+$ cells but not in T cells. (**G**) Killing assay under various conditions as indicated shows reduced killing efficacy of target T cells in the presence of anti–Gzm C Ab (α-Gzm C). Glomeruli-infiltrating CD8αα$^+$RT1B/D$^+$ Ly49s$^+$ cells (G CD8αα$^+$) were used as killing effectors and pCol(28–41)-specific T cells as targets. Killing is expressed as percentage of CFSE-labeled target T cells in control wells without killing effectors. Three independent experiments were conducted with similar results. A one-way ANOVA with a Tukey posttest was performed. $*p < 0.05$, $**p < 0.01$, $***p < 0.001$. G, glomeruli-infiltrating cell; P, PBMCs; *Pfr*, perforin.

(Fig. 5B). Both T cell populations expressed most of the 26 non-classic MHC-I RT1C/E, M/N, and S/T genes, with RT1CE16 being the highest (Fig. 5A). However, glomeruli-infiltrating pan T cells showed a significantly higher level of RT1CE16 than did PBMC pan T cells. Elevated level of expression of RT1CE16 in glomeruli-infiltrating T cells was further confirmed by both RT-PCR and qPCR (Fig. 5C, 5D). We asked whether activation led to upregulation of RT1CE16 in T cells, which made them more susceptible to

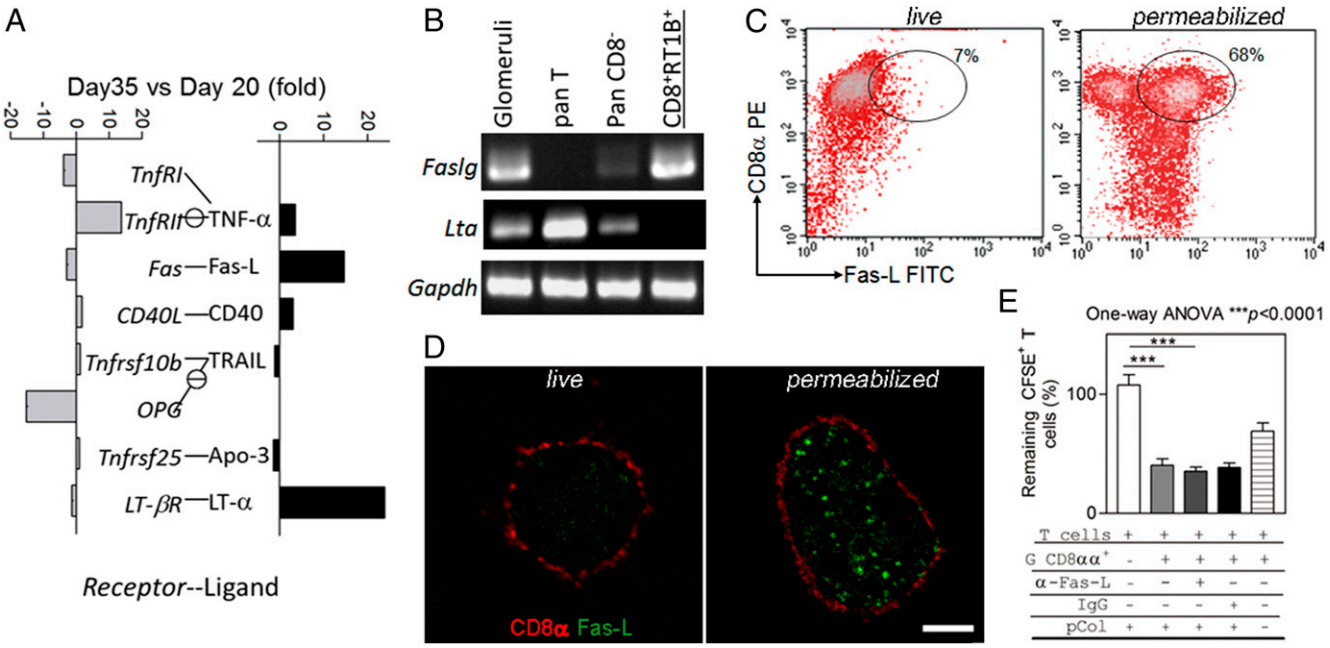

FIGURE 4. CD8αα$^+$RT1B/D$^+$Ly49s6$^+$ cells express intracellular Fas-L. (**A**) qPCR array for apoptosis pathway on glomerular mRNAs at early inflammation (day 20 postimmunization) and T cell apoptosis peak (day 35) of immunized WKY rats; apoptosis-inducing receptors and ligands are shown separately and paired; expression of each gene is expressed as fold changes between day 20 and day 35; note that significant increases are seen in both *Faslg* and *Lta*. (**B**) RT-PCR shows the detection of a high level of *Faslg* mRNA in the isolated glomeruli-infiltrating CD8αα$^+$RT1B/D$^+$Ly49s$^+$ cells (CD8$^+$RT1B$^+$), but no *Lta* expression was detected. (**C**) Two-color flow cytometry on isolated glomeruli-infiltrating CD8αα$^+$RT1B/D$^+$Ly49s6$^+$ cells for the detection of Fas-L; permeabilized cells showed a Fas-L$^+$CD8α$^+$ population (gated). (**D**) Immunofluorescence shows intracellular Fas-L (green) in a permeabilized CD8αα$^+$RT1B/D$^+$ cell (red) (right panel), but not in a live one (left panel). Scale bar, 3 μm. (**E**) Killing assay shows that addition of Fas-L Ab (α-Fas-L) did not inhibit CD8αα$^+$RT1B/D$^+$Ly49s6$^+$ cell–mediated killing of pCol(28–40)-specific T cells. Three independent experiments were conducted with similar results. A one-way ANOVA with a Tukey posttest was conducted. $***p < 0.001$.

Downloaded from http://www.jimmunol.org/ by guest on February 26, 2022

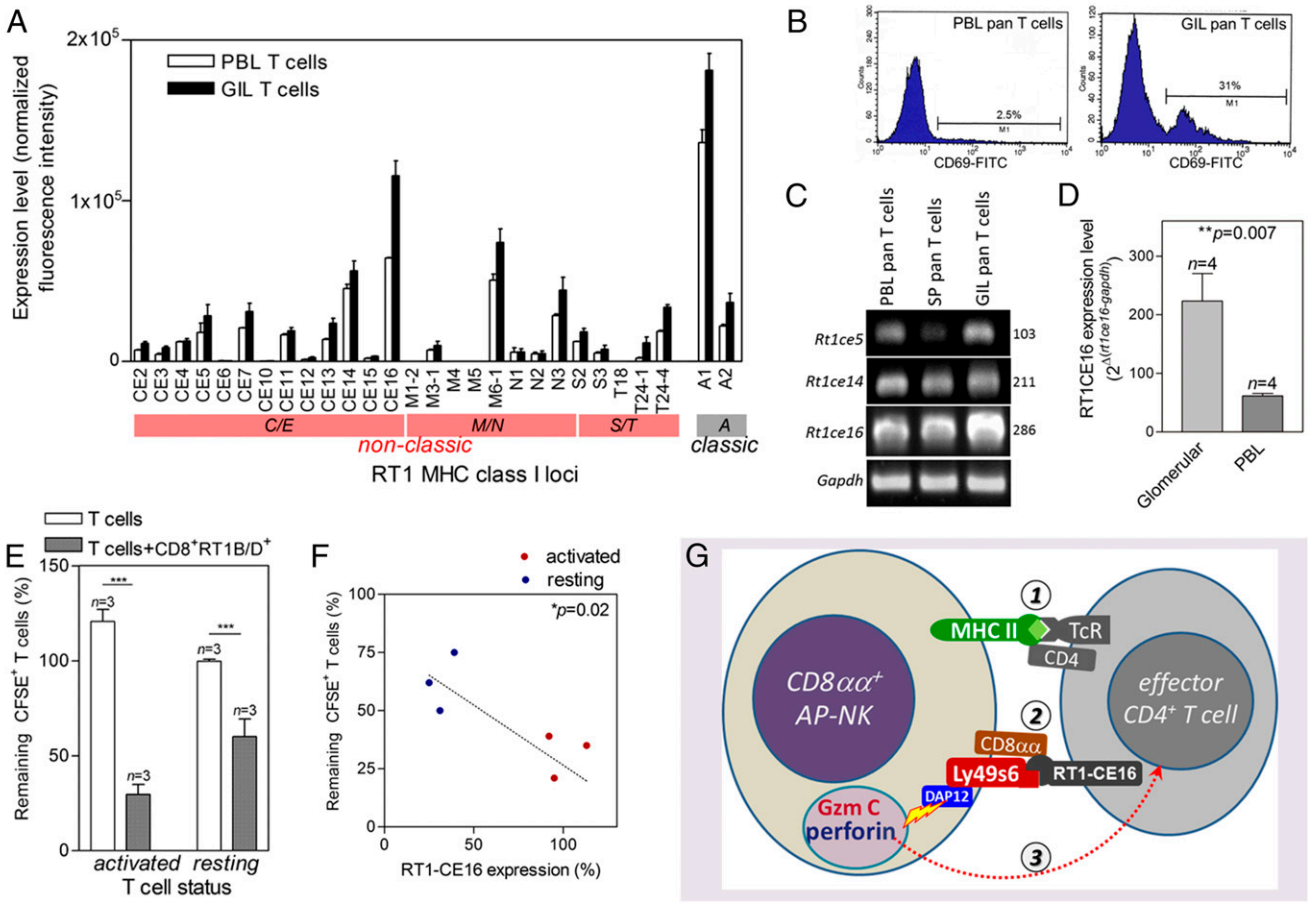

FIGURE 5. Activated autoreactive T cells with an elevated level of RT1CE16 are more susceptible to killing by CD8αα$^+$RT1B/D$^+$Ly49s6$^+$ cells. (**A**) Summary of classic (RT1A) and nonclassic (RT1C/E, M/N, and S/T) MHC-I gene cluster expression pattern in PBMC (P) and glomeruli-infiltrating (GIL) T cells; the expression level is normalized intensities in the DNA microarray (n = 4). (**B**) Flow cytometry shows detection of T cell activation marker CD69 in PBL pan T cells or glomeruli-infiltrating T cells as indicated. (**C**) Conventional RT-PCR detection of representative nonclassic MHC-I genes in PBL, splenic (SP), and glomeruli-infiltrating (GIL) T cells. (**D**) qPCR detection of *Rt1ce16* expression in glomeruli-infiltrating or PBL T cells. Relative expression levels to the housekeeping gene *Gapdh* are shown. (**E**) Summary of susceptibility of T cells to CD8αα$^+$RT1B/D$^+$Ly49s6$^+$ cell–mediated killing. Killing efficacy is expressed as percentage of remaining CFSE-labeled target T cells. T cells alone were used as a control. (**F**) Correlation between RT1CE16 expression level in resting and activated pCol(28–40)-specific T cell lines and their susceptibilities to CD8αα$^+$RT1B/D$^+$Ly49s6$^+$ cell–mediated killing; RT1CE16 expression levels were measured by qPCR and are expressed as the percentage of an average for activated T cells; linear progression was calculated; each sample was duplicated. (**G**) Schematic diagram depicts three-step killing of autoreactive T cells by CD8αα$^+$RT1B/D$^+$Ly49s6$^+$ cells (renamed to CD8αα$^+$ AP-NK cell). Step 1: Coupling of CD8αα$^+$ AP-NK cell with effector autoreactive T cell through its Ag presentation. Step 2: Binding of Ly49s/CD8αα on CD8αα$^+$ AP-NK cell to RT1CE16 on the T cell. Step 3: DAP12-mediated release of granule cytotoxic proteins Gzm C and perforin from the CD8αα$^+$ AP-NK cell, which induce apoptosis in the target T cell.

CD8αα$^+$RT1B$^+$Ly49s6$^+$ cell–induced apoptosis. Resting or activated T cells from three pCol(28–41)-specific autoreactive T cell lines were used for the determination of their RT1CE16 expression with qPCR. First, activated T cells showed a much higher susceptibility to CD8αα$^+$RT1B$^+$Ly49s6$^+$ cell–mediated apoptosis than did resting T cells (Fig. 5E). Interestingly, the activated T cells also showed a much higher expression level of RT1CE16 than did the resting T cells (Fig. 5F). Susceptibility to apoptosis was positively correlated to RT1CE16 expression level (Fig. 5F). This correlation suggests that RT1CE triggered Ly49s6-mediated degranulation.

Discussion

The CD8αα$^+$RT1B/D$^+$Ly49s6$^+$ cell mediates a unique immune tolerance by killing effector T cells in the autoimmune target

We have previously reported the CD8αα$^+$RT1B/D$^+$Ly49s6$^+$ cell as a CD8αα$^+$RT1B/D$^+$ DC-like cell. This cell actively infiltrates inflamed autoimmune target tissue and further induces apoptosis in effector T cells in a rat model for autoimmune glomerulonephritis (13, 14). As a result, an ongoing autoimmune inflammation in the target is terminated at an early stage without any significant impact on the host (12). Although Ag presentation is a critical step leading to T cell apoptosis, it was not clear which molecule/pathway in this cell actually induced T cell apoptosis. In this study, we not only reconfirmed the presence of Ag processing/presenting pathways, but we also revealed complicated cytotoxic mechanisms identical to the Ly49s$^+$ subset of NK cells in this cell. This cell especially expressed killing stimulatory receptor Ly49s6 with nonclassic MHC-I RTCE16 on T cells as a ligand. Cytotoxicity by this cell was eventually mediated by granular cytolytic protein Gzm C, as Ab to Gzm C significantly inhibited its cytotoxicity on T cells. Our results, together with our previous findings, led to the following scenario (Fig. 5G): the CD8αα$^+$RT1B/D$^+$Ly49s6$^+$ cells actively infiltrate inflamed target tissue, and as a professional APC, they process and present local autoantigens to autoreactive effector T cells, leading to coupling between the two. Ly49s6 and CD8αα on this cell serve as killing stimulatory receptors/coreceptors; their binding to nonclassic MHC-I RT1CE16 on target T cells following the coupling triggers Gzm C–mediated

Downloaded from http://www.jimmunol.org/ by guest on February 26, 2022

cytotoxicity. To our knowledge, only a few, if any, known immune tolerance mechanisms act on a pre-existing autoimmune inflammation. In summary, the CD8αα$^+$RT1B/D$^+$Ly49s6$^+$ cell recognizes target T cells as an APC, and it further kills the target in an identical way to an Ly49s$^+$ NK cell. Thus, this is an NK-like cell with Ag-presenting capacity. For a more accurate description of its unique dual functions, we renamed it a CD8αα$^+$ Ag-presenting NK-like (AP-NK) cell (Fig. 5G).

The CD8αα$^+$ AP-NK cell is a novel immune cell with dual functions of an APC and NK cell

Both professional APC function and NK toxicity of the CD8αα$^+$ AP-NK cell were required for the selective elimination of effector autoreactive T cells. Several immune cells with dual functions have been reported. However, they are functionally and phenotypically different from the CD8αα$^+$ AP-NK cell. Inhibitory Ly49 receptors have been detected on a cell of the myeloid lineage in mice as a trafficking regulator (26). Because these cells lack any NK cytotoxic machineries, they are not truly dually functional. A CD4$^+$CD8$^+$ macrophage is capable of killing tumor cells with an NKG2D–Gzm B-dependent mechanism (27). Except for its phenotypic and functional differences from the CD8αα$^+$ AP-NK cell, it remains unclear whether this cell is a professional APC and whether both its APC function and NK-like cytotoxicity are required to kill tumors. A special killer DC in spleen has been identified (28). This cell first displays an NK-like capacity with expression of NKG2D/DAP12, and it subsequently differentiates into a DC with a loss of NKG2D/DAP12 and diminished killing capacity (28). Thus, its NK and APC function are sequential but not simultaneous as seen in CD8αα$^+$ AP-NK cells. Exact function of this killer DC remains unclear but may provide a link between innate and adaptive immunity. A splenic CD8$^+$ DC has been reported to induce T cell apoptosis with Fas-L (29). Although it seems that APC function is required for recognition of T cells, the killing mechanism is not through the NK killing receptor. Thus, the CD8αα$^+$ AP-NK cells are a new type of immune cells with dual functions of professional APC and NK cell cytotoxicity.

What is the lineage of the CD8αα$^+$ AP-NK cells?

Dual functions of the CD8αα$^+$ AP-NK cells raise an interesting question regarding their lineage. Our earlier studies showed that the cells were derived from bone marrow and were most likely a phagocytic lineage, as they were adhesive, morphologically resembled DCs after culture, and expressed professional APC-associated genes such as MHC-II and invariant chain (14, 15). However, our observations in this study suggested otherwise, as the cell possesses a set of NK cytotoxicity–related molecules, from NK killing receptors, DAP12, and Gzms/perforin to Fas-L. However, most of these molecules are not NK specific, and they may also be expressed by other immune cells (26–29). It is known that DCs can express some Gzms. In mice, myeloid cells express certain Ly49 isoforms. Myeloid cells in mice and humans express DAP12. Thus, it is not sufficient to conclude their NK lineage merely based on the expression of these molecules. Alternatively, many recent studies explored whether NK cells express MHC-II as an APC in various species. However, the matter still remains inconclusive. So far as we know, expression of MHC-II by rat NK cells has not been reported. A recent study has reported that decidua basalis NK cells can resemble the morphology of DCs after differentiation into an isoform due to splice variants of the killing receptors (30). The killer DC as described above turns out to be a type of an activated NK cell (31). Thus, it cannot be ruled out that the CD8αα$^+$ AP-NK cell is of the NK lineage with the addition of an Ag processing/presenting apparatus. More studies are needed.

Unique cytotoxic machinery in the CD8αα$^+$ AP-NK cell

Although the CD8αα$^+$ AP-NK cell possesses similar cytotoxic machinery to Ly49s$^+$ NK cells, there are some differences. First, granule cytolytic proteins in NK and CD8$^+$ T cells are mainly Gzm A and B. Alternatively, they were predominantly Gzm C in the CD8αα$^+$ AP-NK cells. Gzm C is much less known. In fact, it remains controversial whether natural Gzm C is a monomer or homodimer or whether it has any function beyond allogeneic rejection (32–34). An x-ray crystallography on native Gzm C revealed it to be a homodimer (21). Because homodimeric configuration seals its catalytic site, Gzm C needs to be converted to be active (21). Our results supported homodimer configuration. This self-locking mechanism may be necessary to minimize collateral damage during killing of effector autoreactive T cells. Second, Ly49 is among many NK receptors with MHC-I as ligands. These NK receptors are largely killing inhibitory as a safeguard for self cells. In contrast, killing stimulatory receptors such as NKG2D bind to other ligands to initiate killing (35). Thus, it seems paradoxical why some MHC-I–binding receptors, for example, stimulatory Ly49s, activate killing. Recent studies have revealed unique functions of these killing stimulatory receptors in allogeneic rejection and certain infections (23, 36). Our discovery adds one more function of these MHC-I–binding killing stimulatory receptors in self-immune tolerance: killing "bad" effector autoreactive T cells. Recognition of autoreactive T cells through Ag presentation of the CD8αα$^+$ AP-NK cell, therefore, is necessary to avoid killing other innocent T cells.

Potential significances of the CD8αα$^+$ AP-NK cell

Many tolerance mechanisms prevent autoimmunity/inflammation de novo. Less is known about the tolerance mechanisms following the occurrence of autoimmune inflammation; these mechanisms must be able to contain pre-existing inflammation. The CD8αα$^+$ AP-NK cell–mediated mechanism is one of them. In fact, LEW rats, which are "resistant" to autoimmune glomerulonephritis, do develop disease identical to disease-prone WKY rats (12, 14). However, disease in LEW rats is contained at early stages by the CD8αα$^+$ AP-NK cell, rather than being prevented (12, 13). Owing to a full recovery, the hosts do not experience a significant impact of autoimmune inflammation on their health status. Mechanisms for containing autoimmune inflammation are as critical as those for prevention. Activation of autoreactive T cells during an infection is well known (37, 38). Copresentation of leaked autoantigens with pathogens during an infection by an APC activates autoreactive T cells, which in turn cause autoimmune inflammation at the infection site (39). However, infection rarely causes autoimmunity. Beyond many others, one reason may be that microscale autoimmunity during an infection is contained locally by infiltrating CD8αα$^+$ AP-NK cells. These cells may preferentially kill autoreactive T cells but spare pathogen-specific T cells, because they present much more leaked autoantigens at the infection site. Thus, microscale autoimmunity is subsequently terminated without significant impact on the host. Second, as the CD8αα$^+$ AP-NK cells are able to actively infiltrate inflamed tissue and further terminate a pre-existing autoimmune inflammation, we are asking whether this unique tolerance mechanism may be used for development of immunotherapies for treating pre-existing autoimmune diseases, especially of an inflammatory nature.

Acknowledgments

Global gene expression detection using DNA microarray was performed at the Quantitative Genomics and Microarray Service Center at the University of Texas Health Science Center at Houston. We thank Dr. Tuan Tran for technical help.

Downloaded from http://www.jimmunol.org/ by guest on February 26, 2022

Disclosures

The authors have no financial conflicts of interest.

References

1. Davidson, A., and B. Diamond. 2001. Autoimmune diseases. *N. Engl. J. Med.* 345: 340–350.
2. Condemi, J. J. 1992. The autoimmune diseases. *JAMA* 268: 2882–2892.
3. Ohashi, P. S. 2002. T-cell signalling and autoimmunity: molecular mechanisms of disease. *Nat. Rev. Immunol.* 2: 427–438.
4. Maddur, M. S., P. Miossec, S. V. Kaveri, and J. Bayry. 2012. Th17 cells: biology, pathogenesis of autoimmune and inflammatory diseases, and therapeutic strategies. *Am. J. Pathol.* 181: 8–18.
5. Feldmann, M., and L. Steinman. 2005. Design of effective immunotherapy for human autoimmunity. *Nature* 435: 612–619.
6. Sakaguchi, S., N. Sakaguchi, J. Shimizu, S. Yamazaki, T. Sakihama, M. Itoh, Y. Kuniyasu, T. Nomura, M. Toda, and T. Takahashi. 2001. Immunologic tolerance maintained by $CD25^+$ $CD4^+$ regulatory T cells: their common role in controlling autoimmunity, tumor immunity, and transplantation tolerance. *Immunol. Rev.* 182: 18–32.
7. Morel, P. A., M. Feili-Hariri, P. T. Coates, and A. W. Thomson. 2003. Dendritic cells, T cell tolerance and therapy of adverse immune reactions. *Clin. Exp. Immunol.* 133: 1–10.
8. Rutella, S., S. Danese, and G. Leone. 2006. Tolerogenic dendritic cells: cytokine modulation comes of age. *Blood* 108: 1435–1440.
9. Setiady, Y. Y., P. Pramoonjago, and K. S. Tung. 2004. Requirements of NK cells and proinflammatory cytokines in T cell-dependent neonatal autoimmune ovarian disease triggered by immune complex. *J. Immunol.* 173: 1051–1058.
10. Albert, L. J., and R. D. Inman. 1999. Molecular mimicry and autoimmunity. *N. Engl. J. Med.* 341: 2068–2074.
11. Horwitz, M. S., L. M. Bradley, J. Harbertson, T. Krahl, J. Lee, and N. Sarvetnick. 1998. Diabetes induced by Coxsackie virus: initiation by bystander damage and not molecular mimicry. *Nat. Med.* 4: 781–785.
12. Robertson, J., J. Wu, J. Arends, C. Zhou, H. E. Adrogue, J. T. Chan, and Y. Lou. 2008. Spontaneous recovery from early glomerular inflammation is associated with resistance to anti-GBM glomerulonephritis: tolerance and autoimmune tissue injury. *J. Autoimmun.* 30: 246–256.
13. Zhou, C., J. Robertson, J. Wu, T. Bartkowiak, K. Parker, J. McMahon, and Y. H. Lou. 2011. Natural recovery from antiglomerular basement membrane glomerulonephritis is associated with glomeruli-infiltrating $CD8\alpha^+CD11c^+$MHC class-II^+ cells. *Am. J. Nephrol.* 34: 519–528.
14. Wu, J., C. Zhou, J. Robertson, C. C. Y. Weng, M. L. Meistrich, R. C. Tailor, and Y. H. Lou. 2010. Identification of a bone marrow-derived $CD8\alpha\alpha^+$ dendritic cell-like population in inflamed autoimmune target tissue with capability of inducing T cell apoptosis. *J. Leukoc. Biol.* 88: 849–861.
15. Wu, J., C. Zhou, J. Robertson, C. Carlock, and Y. H. Lou. 2014. Peripheral blood $CD8\alpha\alpha^+CD11c^+$MHC-II^+CD3^- cells attenuate autoimmune glomerulonephritis in rats. *Kidney Int.* 85: 1078–1090.
16. Wu, J., H. Cherwinski, T. Spies, J. H. Phillips, and L. L. Lanier. 2000. DAP10 and DAP12 form distinct, but functionally cooperative, receptor complexes in natural killer cells. *J. Exp. Med.* 192: 1059–1068.
17. Warren, H. S., and M. J. Smyth. 1999. NK cells and apoptosis. *Immunol. Cell Biol.* 77: 64–75.
18. Kveberg, L., P. Jiménez-Royo, C. Naper, B. Rolstad, G. W. Butcher, J. T. Vaage, and M. Inngjerdingen. 2010. Two complementary rat NK cell subsets, $Ly49s3^+$ and NKR-$P1B^+$, differ in phenotypic characteristics and responsiveness to cytokines. *J. Leukoc. Biol.* 88: 87–93.
19. Nylenna, O., C. Naper, J. T. Vaage, P. Y. Woon, D. Gauguier, E. Dissen, J. C. Ryan, and S. Fossum. 2005. The genes and gene organization of the Ly49 region of the rat natural killer cell gene complex. *Eur. J. Immunol.* 35: 261–272.
20. Naper, C., K. Z. Dai, L. Kveberg, B. Rolstad, E. C. Niemi, J. T. Vaage, and J. C. Ryan. 2005. Two structurally related rat Ly49 receptors with opposing functions (Ly49 stimulatory receptor 5 and Ly49 inhibitory receptor 5) recognize nonclassical MHC class Ib-encoded target ligands. *J. Immunol.* 174: 2702–2711.
21. Kaiserman, D., A. M. Buckle, P. Van Damme, J. A. Irving, R. H. Law, A. Y. Matthews, T. Bashtannyk-Puhalovich, C. Langendorf, P. Thompson, J. Vandekerckhove, et al. 2009. Structure of granzyme C reveals an unusual mechanism of protease autoinhibition. *Proc. Natl. Acad. Sci. USA* 106: 5587–5592.
22. Lettau, M., M. Paulsen, D. Kabelitz, and O. Janssen. 2008. Storage, expression and function of Fas ligand, the key death factor of immune cells. *Curr. Med. Chem.* 15: 1684–1696.
23. Shegarfi, H., K. Z. Dai, M. R. Daws, J. C. Ryan, J. T. Vaage, B. Rolstad, and C. Naper. 2011. The rat NK cell receptors Ly49s4 and Ly49i4 recognize nonclassical MHC-I molecules on *Listeria monocytogenes*-infected macrophages. *J. Leukoc. Biol.* 89: 617–623.
24. Gao, G. F., B. E. Willcox, J. R. Wyer, J. M. Boulter, C. A. O'Callaghan, K. Maenaka, D. I. Stuart, E. Y. Jones, P. A. Van Der Merwe, J. I. Bell, and B. K. Jakobsen. 2000. Classical and nonclassical class I major histocompatibility complex molecules exhibit subtle conformational differences that affect binding to $CD8\alpha\alpha$. *J. Biol. Chem.* 275: 15232–15238.
25. Roos, C., and L. Walter. 2005. Considerable haplotypic diversity in the RT1-CE class I gene region of the rat major histocompatibility complex. *Immunogenetics* 56: 773–777.
26. Sasawatari, S., M. Yoshizaki, C. Taya, A. Tazawa, K. Furuyama-Tanaka, H. Yonekawa, T. Dohi, A. P. Makrigiannis, T. Sasazuki, K. Inaba, and N. Toyama-Sorimachi. 2010. The Ly49Q receptor plays a crucial role in neutrophil polarization and migration by regulating raft trafficking. *Immunity* 32: 200–213.
27. Baba, T., S. Iwasaki, T. Maruoka, A. Suzuki, U. Tomaru, H. Ikeda, T. Yoshiki, M. Kasahara, and A. Ishizu. 2008. Rat $CD4^+CD8^+$ macrophages kill tumor cells through an NKG2D- and granzyme/perforin-dependent mechanism. *J. Immunol.* 180: 2999–3006.
28. Chan, C. W., E. Crafton, H. N. Fan, J. Flook, K. Yoshimura, M. Skarica, D. Brockstedt, T. W. Dubensky, M. F. Stins, L. L. Lanier, et al. 2006. Interferon-producing killer dendritic cells provide a link between innate and adaptive immunity. *Nat. Med.* 12: 207–213.
29. Süss, G., and K. Shortman. 1996. A subclass of dendritic cells kills CD4 T cells via Fas/Fas-ligand-induced apoptosis. *J. Exp. Med.* 183: 1789–1796.
30. Siewiera, J., J. Gouilly, H. R. Hocine, G. Cartron, C. Levy, R. Al-Daccak, and N. Jabrane-Ferrat. 2015. Natural cytotoxicity receptor splice variants orchestrate the distinct functions of human natural killer cell subtypes. *Nat. Commun.* 6: 10183.
31. Vosshenrich, C. A., S. Lesjean-Pottier, M. Hasan, O. Richard-Le Goff, E. Corcuff, O. Mandelboim, and J. P. Di Santo. 2007. $CD11c^{lo}B220^+$ interferon-producing killer dendritic cells are activated natural killer cells. *J. Exp. Med.* 204: 2569–2578.
32. Getachew, Y., H. Stout-Delgado, B. C. Miller, and D. L. Thiele. 2008. Granzyme C supports efficient CTL-mediated killing late in primary alloimmune responses. *J. Immunol.* 181: 7810–7817.
33. Cai, S. F., T. A. Fehniger, X. Cao, J. C. Mayer, J. D. Brune, A. R. French, and T. J. Ley. 2009. Differential expression of granzyme B and C in murine cytotoxic lymphocytes. *J. Immunol.* 182: 6287–6297.
34. Bailey, N. C., and C. J. Kelly. 1997. Nephritogenic T cells use granzyme C as a cytotoxic mediator. *Eur. J. Immunol.* 27: 2302–2309.
35. Long, E. O., H. S. Kim, D. Liu, M. E. Peterson, and S. Rajagopalan. 2013. Controlling natural killer cell responses: integration of signals for activation and inhibition. *Annu. Rev. Immunol.* 31: 227–258.
36. Sivori, S., S. Carlomagno, M. Falco, E. Romeo, L. Moretta, and A. Moretta. 2011. Natural killer cells expressing the KIR2DS1-activating receptor efficiently kill T-cell blasts and dendritic cells: implications in haploidentical HSCT. *Blood* 117: 4284–4292.
37. Wucherpfennig, K. W. 2001. Mechanisms for the induction of autoimmunity by infectious agents. *J. Clin. Invest.* 108: 1097–1104.
38. Fujinami, R. S., M. G. von Herrath, U. Christen, and J. L. Whitton. 2006. Molecular mimicry, bystander activation, or viral persistence: infections and autoimmune disease. *Clin. Microbiol. Rev.* 19: 80–94.
39. Horwitz, M. S., A. Ilic, C. Fine, E. Rodriguez, and N. Sarvetnick. 2002. Presented antigen from damaged pancreatic β cells activates autoreactive T cells in virus-mediated autoimmune diabetes. *J. Clin. Invest.* 109: 79–87.

Downloaded from http://www.jimmunol.org/ by guest on February 26, 2022